Differential Absorption Flattening Optical Effects Are Significant in the Circular Dichroism Spectra of Large Membrane Fragments†

B. A. Wallace* and C. L. Teeters

Department of Biochemistry and Molecular Biophysics, Columbia University, New York, New York 10032

Received June 16, 1986; Revised Manuscript Received August 1, 1986

ABSTRACT: The circular dichroism spectra of membrane particles are distorted by effects of differential absorption flattening, which are a consequence of the nonrandom distribution of chromophores in these samples. We have shown that this phenomenon is not significant in small unilamellar vesicles with high lipid to protein ratios [Mao, D., & Wallace, B. A. (1984) *Biochemistry 23*, 2667–2673]. It has recently been claimed [Glaeser, R. M., & Jap, B. K. (1985) *Biochemistry 24*, 6398–6401] that absorption flattening effects are also inconsequential in large membrane fragments with high protein concentrations, such as purple membrane sheets. This paper will demonstrate that absorption flattening is significant in these samples and that it causes substantial distortion of the calculated protein secondary structures derived from the uncorrected circular dichroism data.

It has been reported that differential absorption flattening effects result in significant distortions of the circular dichroism (CD)[1] spectra of large membrane particles (Urry, 1972; Wallace & Mao, 1984) but not in the spectra of small unilamellar vesicles (SUVs) with high lipid to protein ratios (Mao & Wallace, 1984). If left uncorrected, these effects result in errors in secondary structures calculated from these data.

In a recent paper, Glaeser and Jap (1985) dispute these conclusions based on their reinterpretation of data from our laboratory (Mao & Wallace, 1984). Since knowledge of these effects is essential to determinations of membrane protein secondary structures by circular dichroism spectroscopy, and since CD has been one of the few methods to date which has provided information on membrane protein structures, it is important to discuss these issues. The source of the confusion is the magnitude of the differential absorption flattening, as determined from comparisons of the spectra of bacteriorhodopsin in purple membranes (PMs), sonicated purple membranes, and SUVs. It was stated in our original work that the magnitudes of the SUV spectra were not expected to be exact but that the method of analysis we used to show the absorption flattening distortion was independent of the absolute magnitude; this was unlike the approach taken by Glaeser and Jap which did require such information. To clarify this issue, we have repeated our SUV and PM circular dichroism experiments, paying careful attention to the magnitudes of the curves. The present experiments unequivocally demonstrate that differential absorption flattening effects are significant in purple membrane sheets at all wavelengths in the far UV. We also demonstrate that knowledge of the magnitude of the curve is not essential for determination of secondary structures by CD, providing an unconstrained, normalized method of analysis is employed. We also systematically show problems that can arise with the use of constrained analyses.

Materials and Methods

Samples. PMs were isolated from *Halobacterium halobium*, and samples were prepared for spectroscopy in deionized water as previously described (Mao & Wallace, 1984). SUVs were prepared from dimyristoylphosphatidylcholine (Calbiochem) as previously described (Mao & Wallace, 1984) with lipid to protein mole ratios of 150:1. SUVs were also prepared without protein present and were used as blanks for the SUV samples in spectroscopic measurements and protein assay determinations.

Protein Concentration Determinations. (*A*) *Quantitative Amino Acid Analyses.* Samples used for spectroscopy were prepared for quantitative amino acid analysis by addition of a known amount of a norleucine standard, followed by lyophilization and hydrolysis. Total protein content was determined, and completion of the hydrolysis reaction was checked by comparison of the amino acid compositions with values calculated from the published sequence for BR (Khorana et al., 1979; Ovchinnikov et al., 1979). The influence of lipid on these analyses was determined by comparisons of equal aliquots of PM samples with and without added lipid. The reproducibility between repeated runs was ~±5%.

(*B*) *Lowry Assays.* For comparisons of the accuracy of assays in estimating protein concentrations for BR in different environments, the method of Lowry et al. (1951) was used in the presence of 0.1% SDS with dark-adapted PMs as the standard.

(*C*) *Extinction Coefficients.* Native PM concentrations were checked spectrophotometrically by using a molar extinction coefficient of 63 000 at 568 nm for dark-adapted samples. The extinction coefficient for BR in SUVs was estimated from the quantitative amino acid analysis determination of concentration and spectroscopic measurements at the 558-nm retinal chromophore peak.

Circular Dichroism Spectroscopy. Spectra were recorded on an AVIV 60DS spectropolarimeter fitted with a variable-position detector. Detector acceptance angles of 90° were used for all specimens to limit differential scattering effects. The instrument was calibrated for optical rotation with *d*-camphorsulfonic acid at both 290 and 192.5 nm and checked with myoglobin. The wavelength was calibrated with benzene vapor to be within ±0.1 nm for all peaks. The wavelength range

† This work was supported by NIH Grants GM27292 and AM31089. B.A.W. is the recipient of a Dreyfus Teacher–Scholar Award.

* Correspondence should be addressed to this author.

[1] Abbreviations: CD, circular dichroism; UV, ultraviolet; PM, purple membrane; SUV, small unilamellar vesicle; BR, bacteriorhodopsin; SDS, sodium dodecyl sulfate; BPTI, bovine pancreatic trypsin inhibitor.

0006-2960/87/0426-0065$01.50/0

scanned for all samples was from 300 to 185 nm, using 0.2-mm path-length cells. The spectra reported are the average of four scans for each sample after subtraction of the appropriate base lines. For each type of preparation, three independent samples were examined.

Calculation Algorithms. Data points were analyzed at 1-nm intervals between 190 and 240 nm by using both a normalized, unconstrained (to sum to unity) fitting procedure (Mao et al., 1982; Magar, 1968) and a constrained procedure which required both the fraction of each type of secondary structure to be positive and the sum of the fractions to equal unity (Himmelblau, 1972; Chang et al., 1978). The reference data set used for both types of analyses was that of Chang et al. (1978). An average helix length of 26 residues was used in the BR analyses, and an average helix length of 13 residues was used in the myoglobin analyses. The sums reported are for the total secondary structures calculated prior to normalization. The normalized root mean square deviation (NRMSD) parameters reported are a measure of the quality of the fit of the calculated secondary structure to the observed CD data (Mao et al., 1982). The R factor is the correspondence between the calculated structure and the X-ray structure and is defined as $|f_c - f_x|/f_x$, where the values of f_c are the fractions of each type of secondary structure calculated from the CD data and the values of f_x are the fractions from the X-ray data.

Results and Discussion

Concentration of BR in SUVs. Amino acid analyses can accurately measure protein concentrations, provided internal standards are used to determine quantitative recovery. In addition, the completeness of hydrolysis can be ascertained for proteins like bacteriorhodopsin with known amino acid compositions. The concentrations of BR in SUVs determined by quantitative amino acid analysis were compared with the concentrations determined by Lowry assay reported earlier and repeated here on similar samples. As was suggested in the previous work (Mao & Wallace, 1984), the concentration of BR in SUVs determined by the Lowry method is too high, thus making the calculated ellipticities too low. The error in the Lowry determination is ~35%, which resulted in an underestimate of the ellipticity by 1.35-fold in the previous work, a value that corresponded well with the unconstrained normalization factor derived from our secondary structure calculations.

Glaeser and Jap have suggested an alternate method of quantitation of BR in SUVs based on the absorbance of the retinal chromophore in the visible region using the extinction coefficient of PMs. However, this peak is very sensitive to environment; we can now calculate the value of the molar extinction coefficient at the 558-nm maximum in SUVs to be approximately 48 000, in comparison to the value of 63 000 at the 568-nm maximum for PMs. If used for the concentration determination, this would have resulted in an overestimate of the ellipticities by 1.3-fold (curiously, this is roughly the inverse of the error resulting from the Lowry determination).

Absorption Flattening Is Significant in Intact and Sonicated Purple Membranes. To accurately demonstrate the magnitude of absorption flattening, we have repeated our CD measurements of PMs, sonicated PMs, and BR in SUVs and used the quantitative amino acid analyses to determine protein concentrations. Figure 1 dramatically demonstrates that there is a significant difference in the magnitudes of the SUV and PM curves at all wavelengths in the far-UV region and that the relative flattening effects range from 27% at 224 nm to 42% at 193 nm. The sonicated PM and PM spectra have nearly identical magnitudes at 224 nm although slightly different shapes, so the sonicated PM samples must also exhibit significant absorption flattening. These studies confirm our earlier conclusions that absorption flattening is significant for both PM and sonicated samples (Wallace & Mao, 1984).

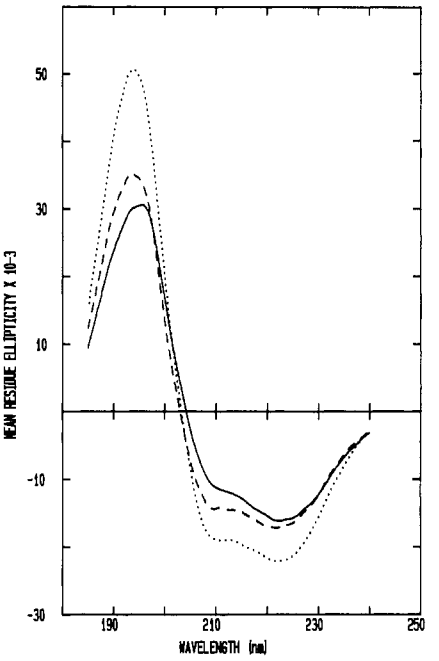

FIGURE 1: Circular dichroism spectra of bacteriorhodopsin in SUVs (···), in sonicated purple membranes (- - -), and in native purple membrane sheets (—) showing that absorption flattening occurs in native and sonicated membranes at all wavelengths in the far-UV region.

Estimate of Absorption Flattening according to the Method of Gordon and Holzwarth. It has been shown that membranes, because of their particulate nature, exhibit flattening of both their absorbance and circular dichroism spectra and that if these artifacts are not corrected for, the estimated protein secondary structures derived from such spectra will be grossly in error (Urry, 1972; Schneider et al., 1970; Wallace & Mao, 1984). Absorption flattening is a consequence of the nonrandom distribution of chromophores within a sample. This occurs in membrane samples because although the protein chromophores are randomly distributed within the membranes, which, in turn, are randomly distributed within the solution, the proteins are sequestered in the discrete regions of the membranes.

Theoretical methods for estimating the extent of absorbance flattening by suspensions of solid cubes and spheres (Duysens, 1956), and of spherical shells (Gordon & Holzwarth, 1971), have been presented. Gordon and Holzwarth have also examined the differential flattening of the circular dichroism spectra for suspensions of such particles. More recently, we (Teeters et al., 1986) have extended the theory to include membrane sheets.

The extent of absorption flattening is a function of the concentration of absorbers in each particle. Particles that absorb more will exhibit more absorption flattening. Absorption flattening of circular dichroism at a given wavelength is defined by the value Q_B, which is the ratio of the sample signal to the signal of a solution which exhibits no flattening. The quantity A_{sol}/qm is defined by Gordon and Holzwarth as the variable upon which absorption flattening is dependent. A_{sol} is the absorbance of an ideal solution of the absorbing species, and qm is a parameter representing the particulate

nature of the sample. The value of qm is related to N, the concentration of particles, by the expression $qm = Ns_ph$, where h is the path length and s_p is the area of the particle projected onto the face of the cuvette (Gordon & Holzwarth, 1971).

In addition to defining the value of A_{sol}/qm, the particle geometry also defines how Q_B is related to A_{sol}/qm. Gordon and Holzwarth (1971) show that spherical shells and solid spheres are distinctly different in their flattening characteristics. Sonicating large solid particles will reduce flattening by decreasing the particle size. However, the absorption flattening exhibited by a shell is insensitive to radius when the radius of the shell is much larger than its thickness. A_{sol}/qm depends on the thickness. This dependence on thickness is also found for sheets (Teeters et al., 1986). As a result, sonication cannot produce significant relief from absorption flattening for spherical shells or sheets when the thickness is unaltered.

It has been estimated that the secondary structure of BR in PM is approximately 80% α-helix (Henderson & Unwin, 1975; Engelman et al., 1980; Nabedryk et al., 1985). A protein with this helical content should have an ellipticity of approximately 26 700 at 224 nm (Chang et al., 1978; Mao & Wallace, 1984); however, the measured value for PMs at 224 nm is 16 200. This results in a Q_B of 0.61 (16 200/26 700) if the observed attenuation of the CD signal relative to the theoretical value is totally due to absorption flattening. For large sheets, this corresponds to an A_{sol}/qm of 0.35 (Teeters et al., 1986).

In PMs, BR molecules are close packed in crystalline arrays. Incorporation into SUVs alters the local concentration by dispersing the proteins with lipid, resulting in a larger distance between proteins and hence a lower concentration (Cherry et al., 1978). On the basis of the relative surface areas occupied by BR and lipids, it can be calculated that the protein concentration in the plane of the SUV membranes decreases ~11-fold relative to that in PM and in sonicated PMs, although the overall concentration of protein in the solution is unchanged. This means that A_{sol} for BR in SUVs would be decreased by a factor of 0.09. The effective thickness of an SUV is approximately twice that of a PM sheet (Teeters et al., 1986). This would decrease the value of m 2-fold relative to that for PMs, resulting in an overall change in A_{sol}/qm by a factor of 0.18. Using the value of A_{sol}/qm for PMs described above, we found that SUVs should then have an A_{sol}/qm of 0.06 and a Q_B of 0.88 at 224 nm. Consequently, the flattening of PMs relative to SUVs at 224 nm is expected to be 0.6/0.88 or a diminution of 32% in magnitude, similar to the 27% decrease observed.

Sonication does not disrupt the crystalline arrays. Therefore, the local concentration of protein chromophores is unaltered in sonicated PMs relative to PMs, and so A_{sol}/qm will be unchanged. The alteration in geometry of the particles will result in a change in the relationship of Q_B to A_{sol}/qm. Sonicated PMs are sheets with diameters roughly equal to 5 times their thickness. A suspension of particles of this geometry would result in a Q_B of approximately 0.69 (Teeters et al., 1986). The observed flattening of sonicated PMs at 224 nm relative to the theoretical spectrum is 0.64, a close correspondence. A normal distribution in the size of the sonicated particles (with some of the particles larger than stated) could easily account for the slightly lower observed Q_B. Therefore, the experimental observation that PMs and sonicated PMs are flattened to roughly the same extent is in accord with theoretical predictions (0.61 vs. 0.69).

To understand why Glaeser and Jap predicted a result that is inconsistent with the data, it is necessary to examine the assumptions of their model. They attempted to use the method of Gordon and Holzwarth (1971) to estimate the extent of absorption flattening by treating PM sheets as spherical shells for estimates of the dependence of Q_B on A_{sol}/qm, but treating the sheets as solid spheres or cubes for the estimate of the size dependence of qm. They suggested that if absorption flattening occurs, the Q_B for sonicated membrane sheets should be 5 times that of intact membranes. Since there is only a slight diminution in signal between sonicated and intact membranes, they asserted that there was no significant absorption flattening in either sample. This conclusion is erroneous since, as demonstrated, absorption flattening is significant for both membrane patches and sonicated membranes. As Gordon and Holzwarth showed for spherical shells, and which is also true for sheets, these shapes should be treated as two-dimensional objects. The membrane thickness does not change upon sonication; only the diameter changes. Therefore, N is inversely proportional to the square (not to the cube as assumed by Glaeser and Jap) of the sheet diameter. Since the area s_p is proportional, to the square of the sheet diameter, the change in the values of N and s_p cancels, and qm remains constant when PM samples are sonicated. Since A_{sol} does not change when the local concentration of absorbing species is not altered, A_{sol}/qm will remain constant. The only minor change in Q_B between PMs and sonicated samples will be due to the change in particle geometry. Hence, significant differences in flattening should be observable between PMs and SUVs, but not between PMs and sonicated PMs, as was shown experimentally.

Comparisons of SUV and Detergent-Solubilized BR. The process of incorporation of BR into vesicles could result in a change in protein conformation; the difference in the waveforms of the SUV, and PM and sonicated PM curves, has been suggested to be evidence of this (Glaeser & Jap, 1985). However, the difference is actually a direct consequence of differential absorption flattening, which depresses the 193- and 208-nm maxima relative to the 224-nm peak in both the PM and sonicated samples. The differences between the spectra of the SUV and the sonicated and PM samples are a demonstration that flattening does occur, rather than being an indication that the incorporation method is distorting the structure. Indeed, spectra of native PMs which have been corrected for these effects are virtually superimposable on the spectra of BR in SUVs (Wallace & Mao, 1984).

It has also been suggested (Glaeser & Jap, 1985) that detergent-solubilized BR should be the same as BR in SUVs, and so should result in the same calculated secondary structure. However, several comparisons suggest that these types of samples are not equivalent. In the visible range, the retinal chromophore absorbs at 558 nm for SUVs and at 552 nm for octyl glucoside solubilized samples as compared with 568 nm for native PM, suggesting a slight alteration in the region around the retinal for both solubilized and SUV samples. This region is not necessarily a sensitive measure of the backbone conformation. Rather, it reflects the retinal environment, which is likely influenced more by the side-chain positions than by the secondary structure. Furthermore, the large 568- to 412-nm shift during the photocycle is a consequence of protonation/deprotonation of the retinal and not of changes in the polypeptide backbone structure, as has been suggested (Glaeser & Jap, 1985).

The far-UV region of the spectrum is probably the best indicator of the integrity of the protein backbone. In this region, the unpolarized peak maxima for SUVs and native PMs are identical (193 nm), while the peak for the deter-

Table I: Correspondence of Calculated and Observed Data for Different Types of Analyses

protein	method	helix	sheet	turn	random	sum	NRMSD	R
myoglobin	normalized	78	1	4	17	1.0	0.030	0.04
	unnormalized	78	1	4	17	1.0	0.030	0.04
	constrained	76	4	3	17	1.0	0.030	0.10
subtilisin	normalized	33	25	11	31	1.0	0.024	0.34
	unnormalized	19	14	7	18	0.6	0.024	0.47
	constrained	15	57	5	24	1.0	0.231	0.93
adenyl kinase	normalized	57	10	12	22	1.0	0.050	0.19
	unnormalized	48	8	10	18	0.8	0.050	0.19
	constrained	47	23	9	21	1.0	0.061	0.34
RNase S	normalized	14	53	8	25	1.0	0.066	0.32
	unnormalized	20	73	11	35	1.4	0.066	0.65
	constrained	23	33	14	30	1.0	0.184	0.28
nuclease	normalized	26	26	12	36	1.0	0.032	0.33
	unnormalized	28	28	13	39	1.1	0.032	0.33
	constrained	29	21	13	38	1.0	0.040	0.28
cytochrome *c*	normalized	45	0	26	29	1.0	0.088	0.16
	unnormalized	55	0	32	35	1.2	0.088	0.24
	constrained	48	0	24	28	1.0	0.130	0.18
papain	normalized	27	4	16	54	1.0	0.116	0.25
	unnormalized	29	4	17	59	1.1	0.116	0.30
	constrained	28	0	16	57	1.0	0.122	0.31
BPTI	normalized	2	57	0	41	1.0	0.209	0.58
	unnormalized	4	98	0	71	1.7	0.209	1.27
	constrained	8	33	0	60	1.0	0.312	0.47
elastase	normalized	0	47	7	46	1.0	0.247	0.62
	unnormalized	0	47	7	46	1.0	0.247	0.62
	constrained	0	46	7	47	1.0	0.248	0.64

gent-solubilized sample is found at 190 nm, suggesting some distortion in structure. This 3-nm shift in the UV region not only is a consequence of the transitions of the backbone, and is thus a direct reflection of the secondary structure, but also represents, in terms in energy, approximately 3 times the effect of the wavelength shift in the visible region, and therefore may be more structurally significant. Furthermore, despite the implication that the detergent-solubilized samples are fully functional, this remains unproven since those samples cannot be characterized for light-driven proton pump activity. SUV samples were shown to be highly active for this function. Finally, incorporation of BR into SUVs was not preceded by detergent solubilization (Mao & Wallace, 1984), so the suggestion that the molecules in SUVs had been exposed to the effects of detergent solubilization is unfounded.

Comparisons of Normalized and Constrained Methods of Analysis. The normalized unconstrained method of analysis was chosen to show the distortion in the calculated secondary structures derived from the CD data of samples which exhibited flattening. This method of analysis is dependent on the shape, but not the magnitude, of the curve. However, constrained analyses depend on both these parameters. It has been suggested (Glaeser & Jap, 1985) that the latter method will more accurately determine secondary structures from CD data. In order to investigate the relative merits of different algorithms for calculating secondary structure, we need to introduce two types of parameters as objective means for evaluation. They are NRMSD, which is the correspondence between calculated and observed data, and R factor, which is the correspondence between the calculated structure and the X-ray structure. We have evaluated normalized, unconstrained, and constrained procedures by calculating and comparing these parameters using data for several soluble proteins. Glaeser and Jap suggested that normalization will produce poorer results than the unnormalized solution. As can be seen from Table I, for all the proteins tested, neither the fits nor the R factors of the unnormalized (unconstrained) solutions were better than those of the corresponding normalized solutions. Only in cases where the sums were ~ 1, were the fits and R factors of the unnormalized procedure as good as those of the normalized solutions. Therefore, the claim that an unnormalized analysis is better seems unfounded.

The relative successes of the normalized (unconstrained) and the constrained procedures should be considered. Naturally, those unconstrained solutions which sum to unity give approximately the same results, fits, and R factors as the constrained procedure (i.e., myoglobin, nuclease, and elastase). For proteins for which the sums differ significantly from 1, the normalized and constrained solutions differ considerably. Table I has been divided between the good (NRMSD <0.1) (top) and poor (>0.1) (bottom) fit categories. Only if NRMSD is low (i.e., <0.1) will the spectra derived from the calculated secondary structures and the experimental data correspond well. This is a necessary (although not sufficient) condition for the calculated secondary structure to be a reasonable indication of the actual secondary structure. Of those with good fits, the normalized and constrained solutions are similar for a number of the proteins, but the normalized is considerably better (lower NRMSD) than the constrained for several. Only for one of the proteins, which is poorly fit (BPTI), does the constrained procedure do better than the normalized.

There is no obvious correspondence of quality of fit (NRMSD) with type of secondary structure, except that those proteins with relatively high random coil contents have the poorest fits. This is not an unreasonable result, as random coil is not a single type of secondary structure with defined ϕ,ψ angles. Surprisingly, there is no strong correlation with helix content; the proteins with good fits range from 14% to 78% helix. Also unexpected was the result that the lowest R factors did not correspond to solutions with sums close to 1, but ranged from 0.6 to 1.4. In summary, these results not only suggest the normalized procedure is at least as good as, or better than, the unnormalized and constrained procedures but also point out the importance of calculating the fit parameters as objective criteria for all spectral analyses.

Dependence of Constrained Secondary Structural Analyses on Concentration Determinations. The magnitude of the CD spectrum can also be an issue for determinations of secondary structures. It can be shown mathematically (Mao, 1985) and

Table II: Constrained vs. Normalized Analyses of Myoglobin (Effect of Concentration Errors)

concn	helix	sheet	turn	random	sum[a]	NRMSD
			Constrained Solutions			
1.00×	0.76	0.04	0.04	0.17	1.0	0.030
0.90×	0.66	0.17	0.01	0.15	1.0	0.034
1.10×	0.82	0.00	0.02	0.16	1.0	0.031
0.65×	0.46	0.39	0.00	0.15	1.0	0.071
			Normalized Solutions			
1.00×	0.78	0.01	0.04	0.17	1.0	0.030
0.90×	0.78	0.01	0.04	0.17	0.9	0.030
1.10×	0.78	0.01	0.04	0.17	1.1	0.030
0.65×	0.78	0.01	0.04	0.17	0.65	0.030

[a] For normalized solutions, this is the sum prior to normalization.

experimentally (see below) that a normalized, unconstrained analysis will yield the correct secondary structures (low R factor) independent of the ellipticity magnitude, provided the fit is good (low NRMSD), since it relies only on the waveform. Constrained analyses rely heavily on the magnitude, and so only give the correct secondary structures when the ellipticities are exact. Neither method provides accurate determinations if the fit is poor. When the correct magnitude is available (and there are no other distortions such as absorption flattening present), both analyses should give similar solutions. This is illustrated in the example given in Table II for myoglobin. Myoglobin was chosen as a test protein because its secondary structure is known and its concentration can be accurately determined by either amino acid analysis or spectroscopy. When the concentration is correct (i.e., 1.0×), both solutions are essentially identical. When the concentrations differ by 10% in either direction (i.e., 0.9× or 1.1×), which is easily possible in most routine concentration determinations, the normalized method gives the correct results, but the constrained results are in error by a significant amount. When the concentration is off by 35% (i.e., 0.65×), similar to the case in our original SUV spectra, the normalized solution still gives the correct result, although the constrained analysis is grossly in error. This example dramatically demonstrates the advantage of the normalized, unconstrained analysis approach—the absolute magnitude is not required to obtain the correct secondary structure results.

While there is no substitute for an accurate determination of protein concentration, it alone is not sufficient to ensure that the magnitude of the CD curve will be correct. Many other factors can contribute to errors in magnitude besides protein concentration (Hennessey & Johnson, 1982). One significant factor is the path length of the cell (small variations in path length are common for the very short path-length sandwich disk cells used for particulate samples). Another important factor, especially for membrane proteins which tend to be hydrophobic and sticky, is loss of material on transfer to the spectrophotometer cell (as an example, for the protein fibronectin, losses of up to 80% on each pipetting have been encountered). These factors could be of considerable consequence if the absolute magnitude of the spectrum were required for the analysis.

Using ellipticities determined from concentrations derived from quantitative amino acid analyses, essentially the same calculated secondary structure is obtained for BR in SUVs as we reported previously (80% helix, 0% sheet). The fit is reasonably good (NRMSD = 0.069), although the sum is somewhat less than unity (0.83% ± 0.05%). This latter value is a direct consequence of the residual absorption flattening present in SUVs which, as described earlier, will depress the magnitude by slightly more than 10%. If this were taken into account, then the constrained analysis would give a similar calculated secondary structure to the normalized, unconstrained analysis.

Secondary Structure of Bacteriorhodopsin. The main purpose of this study was not to determine the secondary structure of bacteriorhodopsin but rather to use this protein as a test system for differential absorption flattening since BR not only exists in large membrane patches with high local protein concentrations but can also be incorporated into SUVs in an active form. Although many studies indicate this protein is predominantly helical, it has been suggested that there is good evidence for a substantial amount of β-sheet (Glaeser & Jap, 1985).

Breton and colleagues (Nabedryk et al., 1985) have repeated our CD spectroscopic studies on native PMs, sonicated PMs, and BR in SUVs, using a different method of analysis of the data. As in our work, but unlike the Jap et al. (1983) study, they failed to find more than 5–9% β-sheet structure.

Jap et al. (1983) cite the 1640 cm^{-1} shoulder in their infrared spectrum as strong evidence for substantial β-sheet. However, Nabedryk et al. (1985) have reexamined these data and shown that this peak is most likely a solvent peak which falls at the same frequency. Since the relative intensity of this peak varies in different preparations (Rothschild & Clark, 1979; Jap et al., 1983; Nabedryk et al., 1985; Earnest & Rothschild, 1986) and does not exhibit polarization, as should an amide I peak, it is likely that this is not due to β-sheet but, rather, tightly bound water retained by the air-dried sheets. Furthermore, in light of the Jap et al. report of β-sheet, Nabedryk et al. (1985) collected polarized IR spectroscopic data and showed that the 1685 cm^{-1} peak shoulder they had originally attributed possibly to be β-sheet is more probably β-turn. The feature giving rise to this peak is oriented parallel, not perpendicular, to the membrane surface, as Jap et al. model the sheets in their diffraction data (see below). Earnest and Rothschild (personal communication) utilized polarized IR spectroscopy with Fourier deconvolution and second-derivative techniques to carefully quantitate the secondary structure of BR in PM sheets. They detected a small amount of β-structure but found it could be attributable to β-turn. Finally, using normal mode analyses, Krimm and Dwivedi (1982) were able to completely account for the IR spectrum without resorting to the presence of β-sheet by including α_{II}-helices.

The major evidence for β-structure has been that derived by Jap et al. (1983) from a reinterpretation of the two-dimensional 3.7-Å projection map obtained (Hayward & Stroud, 1981) by image reconstruction of electron micrographs of PMs. Using this higher resolution map, they attribute β-sheet structures to two of the features that had been suggested to be helices in the 7-Å map of Henderson and Unwin (1975). However, it is difficult to attribute any kind of three-dimensional secondary structure to features in a two-dimensional projection map. Henderson and Unwin and, later, Leifer and Henderson (1983) used complete three-dimensional reconstructions, in which such features can be detected with some certainty. Also, new results, including high resolution data (Henderson et al., 1986), suggest that the phase errors in the reflections in the Hayward and Stroud map are ~86° (where 90° is random) between 3.7- and 5.5-Å resolution, the very region of data that gave rise to the features that Jap et al. have interpreted as sheetlike. This seems to suggest that use of that map may not be valid for modeling. Finally, Jap et al. have attempted to model both helices and sheets into the map density. Even without a reported objective quantitative criterion such as a crystallographic R factor, it can be seen that

the fit is not particularly good for either model. It should also be noted that in the X-ray data on oriented PM sheets (Henderson, 1975; Blaurock, 1975) there existed no evidence for a 4.7–4.8-Å repeat that would be typical of β-sheet. While this is not in itself sufficient to eliminate the β-sheet, it is also suggestive that β-sheets may not be a significant structural motif in this protein.

In summary, these studies have shown that absorption flattening is a significant effect in the CD spectra of membrane patches containing high concentrations of proteins. Our original work stated that the concentration reported for the BR in SUVs was unlikely to be accurate but that this would have no consequence in our calculation of the effects of absorption flattening on the secondary structure since a normalized analysis algorithm was used. To eliminate confusion, we have repeated the experiments and included an accurate analysis of protein concentration. The calculated secondary structures obtained for the SUVs are the same as we originally reported. The large differences in magnitude of the PM and SUV spectra of BR at all wavelengths in the far-UV region demonstrate that differential absorption flattening is a significant effect in the spectra of these large membrane fragments containing high protein concentrations and, if uncorrected, will result in errors in calculated secondary structures. Thus, the conclusions from these studies are identical with those reached in our original paper. As suggested earlier (Mao et al., 1982), this study has also demonstrated the precautions that must be taken in using constrained analyses with indeterminate spectral magnitudes.

ACKNOWLEDGMENTS

We thank M. Gawinowicz of the Protein Chemistry Core Lab for running the quantitative amino acid analyses, Joseph Eccles of CUNY for helpful discussions, and J. T. Yang of the University of California, San Francisco, for providing us with his CD data for a number of soluble proteins.

REFERENCES

Blaurock, A. E. (1975) *J. Mol. Biol. 93*, 139–158.

Chang, C. T., Wu, C.-S. C., & Yang, J. T. (1978) *Anal. Biochem. 91*, 13–31.

Cherry, R. J., Muller, U., Henderson, R., & Heyn, M. P. (1978) *J. Mol. Biol. 121*, 283–298.

Duysens, L. M. N. (1956) *Biochim. Biophys. Acta 19*, 1–12.

Engelman, D. M., Henderson, R., McLachlan, A. D., & Wallace, B. A. (1980) *Proc. Natl. Acad. Sci. U.S.A. 77*, 2023–2027.

Glaeser, R. M., & Jap, B. K. (1985) *Biochemistry 24*, 6398–6401.

Gordon, D. J., & Holzwarth, G. (1971) *Arch. Biochem. Biophys. 142*, 481–488.

Hayward, S. B., & Stroud, R. M. (1981) *J. Mol. Biol. 151*, 491–517.

Henderson, R. (1975) *J. Mol. Biol. 93*, 123–138.

Henderson, R., & Unwin, P. N. T. (1975) *Nature (London) 257*, 28–32.

Henderson, R., Baldwin, J. M., Downing, K. H., Lepault, J., & Zemlin, F. (1986) *Ultramicroscopy 19*, 147–178.

Hennessey, J. P., & Johnson, W. C. (1982) *Anal. Biochem. 125*, 177–188.

Himmelblau, D. M. (1972) *Applied Nonlinear Programming*, p 341, McGraw-Hill, New York.

Jap, B. K., Maestre, M. F., Hayward, S. B., & Glaeser, R. M. (1983) *Biophys. J. 43*, 81–89.

Khorana, H. G., Gerber, G. E., Herlihy, W. C., Gray, C. P., Anderegg, R. J., Nihei, K., & Biemann, K. (1979) *Proc. Natl. Acad. Sci. U.S.A. 76*, 5046–5050.

Krimm, S., & Dwivedi, A. M. (1982) *Science (Washington, D.C.) 216*, 407–408.

Leifer, D., & Henderson, R. (1983) *J. Mol. Biol. 163*, 451–466.

Magar, M. E. (1968) *Biochemistry 7*, 617–620.

Mao, D. (1985) Ph.D. Thesis, Columbia University.

Mao, D., & Wallace, B. A. (1984) *Biochemistry 23*, 2667–2673.

Mao, D., Wachter, E., & Wallace, B. A. (1982) *Biochemistry 21*, 4960–4968.

Nabedryk, E., Bardin, A. M., & Breton, J. (1985) *Biophys. J. 48*, 873–876.

Ovchinnikov, Yu., Abdulaev, N. G., Feigina, M. Yu., Kiselev, A. V., & Lobanov, N. A. (1979) *FEBS Lett. 100*, 219–224.

Rothschild, K. J., & Clark, N. A. (1979) *Science (Washington, D.C.) 204*, 311–312.

Schneider, A. S., Schneider, M.-J. T., & Rosenheck, K. (1970) *Proc. Natl. Acad. Sci. U.S.A. 66*, 793–798.

Teeters, C. L., Eccles, J., & Wallace, B. A. (1986) *Biophys. J.* (in press).

Urry, D. W. (1972) *Biochim. Biophys. Acta 265*, 115–168.

Wallace, B. A., & Mao, D. (1984) *Anal. Biochem. 142*, 317–328.